TOWARDS A FUSION OF SAR-INTERFEROMETRY, GNSS AND PRECISE LEVELLING IN THE UPPER RHINE GRABEN AREA, SOUTHWEST GERMANY

T. Fuhrmann, A. Knöpfler, M. Mayer, A. Schenk, M. Westerhaus, K. Zippelt, and B. Heck

Geodetic Institute, Karlsruhe Institute of Technology, Germany

ABSTRACT

InSAR, GNSS and precise levelling provide a unique database to detect recent displacements of the Earth's surface. Data of all three measurement techniques have been collected in order to gain detailed insight into the horizontal and vertical velocity field of the Upper Rhine Graben (URG) area. This paper presents the database and the processing strategies for the calculation of displacements from InSAR, GNSS and levelling measurements in the URG area. Man-induced surface deformations caused by oil extraction in the Northern URG are investigated serving as a study area for the comparison of techniques. In order to benefit from the advantages of each technique we present a strategy to consistently link the different observation methods in a multi-technique approach.

Key words: Upper Rhine Graben; Recent displacements; InSAR; GNSS; Levelling.

1. INTRODUCTION

As central and most prominent segment of the European Cenozoic rift system, the seismically and tectonically active Rhine Graben is of steady geo-scientific interest [1], [2]. Its southern part, called URG, extends from Basel to Frankfurt and is bounded on the French side by the Vosges Mountains and on the German side by the Black Forest. In the last decades, the URG is characterised by small tectonic movements (< 0.5 mm/a). The URG is considered to be the seismically most active region of Northwest Europe with significant probability for the occurrence of destructive earthquakes [3].

The evolution and neotectonics of the URG have been studied by a consortium of 25 universities and governmental agencies from Germany, France, the Netherlands and Switzerland from 1999 to 2007 in the EUCOR-URGENT project (European Confederation of URG universities – URG Evolution and Neotectonics). At that time, the geodetic efforts were not able to resolve active deformation in the URG area unambiguously, since the available networks and data sets were not dense enough, neither in space nor in time. Today, data from geodetic networks of permanent GNSS sites and repeatedly measured levelling are made available from the national surveying agencies of Germany, France and Switzerland. In addition, SAR acquisitions from ESA's data archives have been ordered and processed. The joint analysis of data sets obtained by three different geodetic techniques allows for the determination of horizontal and vertical displacements in the URG with unprecedented accuracy and resolution. Precise geodetic information with high spatial and temporal resolution is also essential for researchers and decision makers as the exploration activity in the URG is significantly increasing in the past decades (e. g., geothermal energy, oil, groundwater management).

This paper will firstly introduce our database consisting of InSAR, GNSS and levelling measurements as well as the processing strategies for the estimation of displacements. Sect. 3 presents current results including a comparison of estimates from different techniques in an oil extraction area. Finally, some principal aspects on the fusion of velocity results from InSAR, GNSS and levelling are discussed (Sect. 4).

2. GEODETIC DATABASE

This section presents the three geodetic measurement techniques used for the calculation of the recent velocity field of the URG. Fig. 1 displays the SAR ground tracks, the GNSS network and the levelling lines analysed within our research project. The database and the processing strategies for the determination of displacements are explained separately for InSAR, GNSS and levelling data.

2.1. InSAR

To obtain a high accuracy for line of sight (LOS) displacement rates, ERS-1/2 and Envisat data from ascending and descending orbits covering a period from 1992 to 2000 and 2002 to 2010, resp., are processed using StaMPS (Stanford Method for Persistent Scatterers, [4]). As whole stripes of data along the URG are ordered from ESA's archives, unfocussed raw data is used. The following steps are applied on the raw data for the determination of LOS displacements:

Proc. 'ESA Living Planet Symposium 2013', Edinburgh, UK
9–13 September 2013 (ESA SP-722, December 2013)

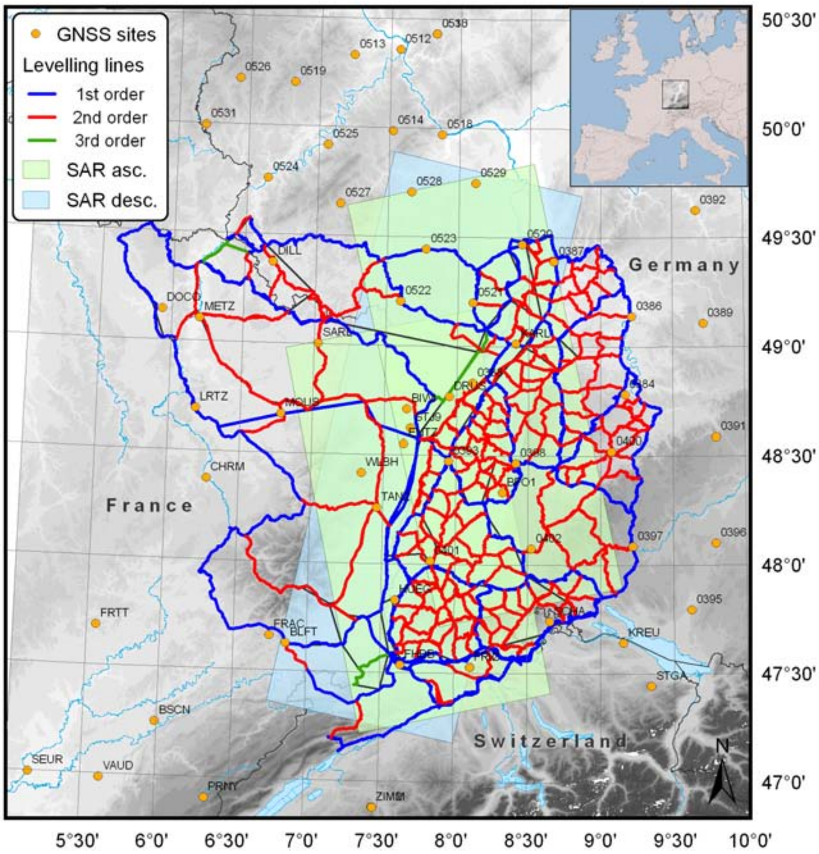

Figure 1. GNSS sites of the Upper Rhine Graben network GURN, ERS-1/2 and Envisat data of track 258, 487 (ascending) and track 294 (descending), and levelling lines of French, German, and Swiss surveying agencies. In the French part, the last complete 1st order levelling was carried out in 1964. In 2001, a traverse from Strasbourg (STJ9) to Nancy (LRTZ) was measured comprising only few former benchmarks. Black straight lines mark historical data measured before the year 1900. The course of the historical lines sometimes differs from later measurements, e. g., north of Strasbourg and west of Basel (FHBB). The levelling benchmarks in these parts cannot be used for displacement estimation.

1. Focussing of raw data to create single look complex images using ROI_PAC [5]
2. Corregistration and formation of interferograms using DORIS [6]
3. Persistent scatterer (PS) analysis using StaMPS [4]

Table 1 gives an overview on the data used in our study. In contrast to the ascending tracks 258 and 487 displayed in Fig. 1, the descending track 294 has a similar orientation as the URG itself and appropriately covers our area of interest. Therefore, we started the InSAR processing with this track. Unfortunately, only few Envisat scenes are available covering the whole stripe. In addition, two ascending tracks will be ordered from ESA's data archive in order to separate the LOS displacements into horizontal and vertical components. As the expected displacements in the URG area are small and the analysed SAR data cover a large area, the separation of atmospheric effects and orbit errors plays an important role in the PS-InSAR processing chain.

Table 1. Usable SAR acquisitions in the URG area.

Satellite	Track	Number of scenes		
		Stripe	North	South
ERS-1/2	294	69	70	69
Envisat	294	16	18	44

2.2. GNSS

The GNSS Upper Rhine Graben network (GURN) was established in September 2008 by the Institut de Physique du Globe de Strasbourg, Ecole et Observatoire des Sciences de la Terre, France and the Geodetic Institute, Karlsruhe Institute of Technology, Germany. Within GURN, the two institutions cooperate in order to carry out geoscientific research in the framework of the transnational project TOPO-WECEP (Western and Central European Platform, [7]). GURN was established as a long-term project in order to derive displacement rates from time series of daily estimated site coordinates based on a highly precise and highly sensitive network of permanently operating GNSS sites [8]. The GURN database starts in 2002 with raw GNSS data from sites located in France and Baden-Württemberg, Germany. A major increase of available sites happened in 2004, when the raw data of sites located in Rheinland-Pfalz, Germany, was made available. Today, GURN consists of approx. 80 sites, most of them capable of tracking GPS and GLONASS signals.

In order to derive daily coordinate estimates at GURN sites, we processed the GNSS data using the Bernese GNSS Software [9]. Most of the coordinate time series are affected by jumps or periodic signals. In order to improve the determination of linear trends, especially for relatively short time series, only sites almost unaffected by seasonal signals are taken into account within this paper. Based on the ITRF2005 network solution and according to [10], residual velocities with respect to an European plate Euler pole estimated purely from the geodetic data set are calculated for each site using local topocentric coordinates (Northing, Easting, Up). To avoid a contamination with artificial jumps due to hardware changes at the GNSS sites, the estimation of linear velocities is restricted to periods of more than two years between known antenna changes. For the estimation approach, a robust linear regression is used, which is nonsensitive to outliers [11]. Further details on the database and the processing strategy are given in [12].

2.3. Levelling

In contrast to InSAR and GNSS data, levelling data is available over a much longer time span in the URG area. Our displacement analysis uses data from the end of the 19th century until today offering the possibility to detect small movements with high accuracy. The data has been measured by the national surveying agencies of Germany, France and Switzerland along lines building closed loops of several 100 km length. The lines of the national networks are divided into different orders depicting the hierarchy of the measurements w.r.t. accuracy and repetition. As the data was measured by different surveying agencies, it is inhomogeneous in space and time (see Fig. 1 and Fig. 2, resp.). Only repeatedly measured levelling benchmarks can be used for the calculation of displacements. Some of the lines consist of only few repeatedly measured benchmarks resulting in a straight connection in Fig. 1.

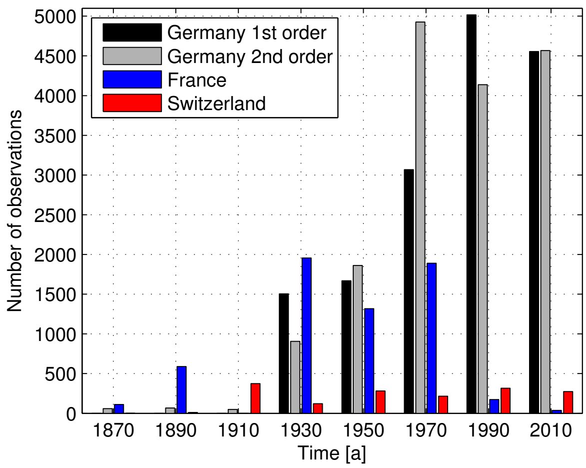

Figure 2. Temporal distribution of levelling observations at repeatedly measured benchmarks for different groups of data.

The easiest way to determine displacements from levelling data is to calculate absolute benchmark heights at one measurement epoch and to subtract them from the heights of a former epoch. This method is valid, if the data was measured at fixed epochs or within short time spans. Our levelling network consists of data from different countries measured at different times. For the displacement analysis of the whole network we therefore apply a kinematic adjustment approach on the data directly yielding vertical displacement rates. The kinematic adjustment models a benchmark height H_j^i using its height at a reference epoch t_0 plus a displacement α_j over time:

$$H_j^i = H_j^0 + \int_{t_0}^{t_i} \alpha_j dt \; . \tag{1}$$

The integral of the movement is approximated using a Taylor expansion which yields

$$H_j^i = H_j^0 + \alpha_{1j} \Delta t_i + \frac{1}{2!} \alpha_{2j} \Delta t_i^2 + \dots \; . \tag{2}$$

In a first step, we assume that all benchmarks have a linear motion expressed by the velocity coefficient α_{1j}. Second, accelerated motions are introduced at benchmarks which show a significant velocity change. To decide whether a second order term has to be introduced or not, a statistical testing on model-related errors is performed [13]. The adjustment is carried out using a Gauss-Markov model with the measured height differences $h_{j,k}^i = H_k^i - H_j^i$ as observations and $\hat{H}$, $\hat{\alpha}_1$ and optionally $\hat{\alpha}_2$ as parameters. Further details on the kinematic adjustment approach including a previous quality check of levelling data using loop misclosures are provided in [12].

For local investigations, in addition to the kinematic analysis a direct comparison of benchmark heights is performed. Fixing the height of a stable starting point of a line, heights are calculated for every benchmark along the line in every measurement epoch. A comparison of the heights at repeatedly measured benchmarks yields vertical displacements w.r.t. the starting point and reference epoch. In contrast to the kinematic approach yielding average displacement rates, this methods resolves for the temporal characteristics of a displacement. It is applied to data in the northern part of the URG for an investigation of man-induced deformation caused by oil extraction.

3. RESULTS

This section presents first results for surface displacements in the URG. For the levelling part, the analysis is finished and therefore presented at the beginning. For InSAR and GNSS, data processing is still in progress and only parts of the whole database are analysed yet. The comparison of results in a test area with larger surface displacements caused by oil extraction demonstrates the potential as well as the limits of each measurement technique.

3.1. Levelling

Vertical displacement rates at levelling benchmarks have been calculated from kinematic network adjustment with an accuracy better than 0.3 mm/a for 90 % of the rates. About 10 % of the vertical rates have been classified as outliers since their value significantly differs from estimates at adjacent benchmarks. Most of the displacement rates are small, 93 % in the range of -0.5 to +0.5 mm/a, concluding that the area generally behaves stable. Results for the region east of the River Rhine are presented in [12]. Fig. 3 shows the average rates for the northern part of the URG area, which is also analysed for the InSAR data in Sect. 3.2. The vertical rates from levelling relate to a reference point in a stable region of the Black Forest.

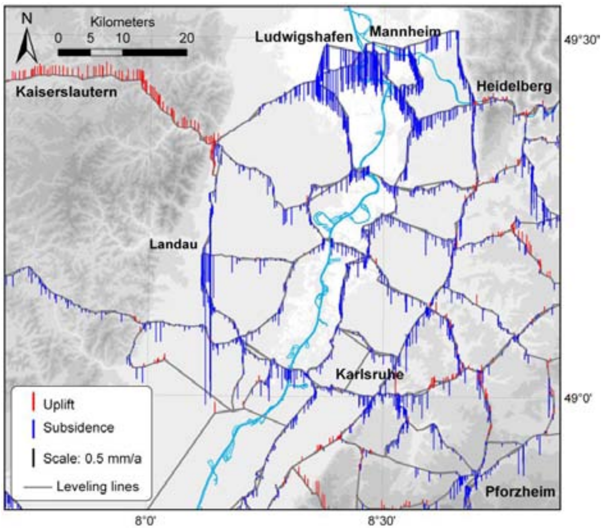

Figure 3. Vertical displacement rates in the Northern URG from kinematic adjustment of levelling data.

Besides a small tectonic uplift northwest of the URG of approx. 0.3 mm/a, some larger non-tectonic displacements are visible in Fig. 3 . The subsidence in the Mannheim/Ludwigshafen region is possibly caused by an extensive groundwater extraction in that industrial area. The strong subsidence signal close to the city of Landau is caused by oil extraction and studied in detail by a comparison of benchmark heights along the levelling line crossing the subsidence area. We will use this local, but relatively strong displacement as a case study to compare the different geodetic methods and to test combination approaches. Fig. 4, top, shows height changes in different measurement epochs starting at a point with a fixed height located south of Landau. All benchmark heights in different epochs are related to the last measurement epoch (2009). Fig. 4, bottom, additionally considers the time between the measurement epochs yielding the velocity of the benchmarks.

Whereas a subsidence with rates up to 5 mm/a is visible in the first measurement epochs, the later epochs reveal a period of significant uplift after 1994. Between 2003 and 2009 the subsidence in the southern part of the levelling

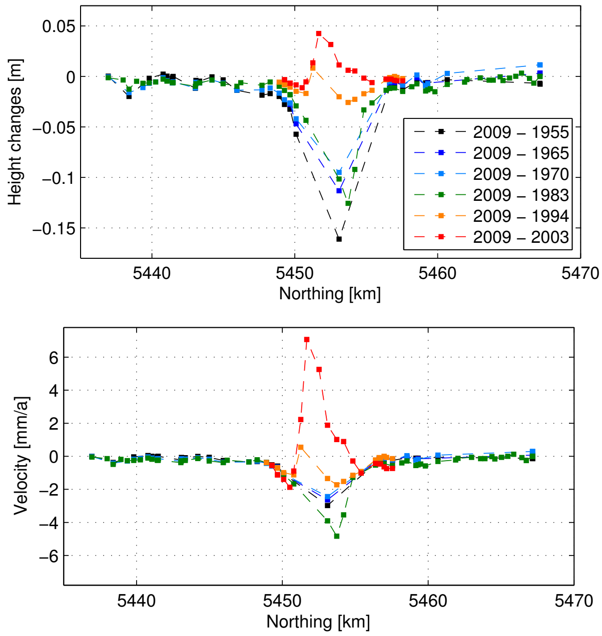

Figure 4. Height changes (top) and velocities (bottom) along a levelling line in the Northern part of the URG w.r.t. the last measurement epoch. The height of the starting point is kept fix.

line transforms into a strong uplift up to 7 mm/a in the centre of the oil extraction area. Subsidence as well as uplift are large enough to be detectable with Envisat data acquired at a similar period, in the years 2003 to 2008.

3.2. InSAR

In the northern part of the URG, 18 Envisat scenes, cf. Tab. 1, are processed using StaMPS. We apply a PS analysis as described in [4] on 17 interferograms w.r.t. a master scene acquired at 2005-08-01. A special focus within the processing is on the estimation of orbit errors and atmospheric signals. Besides the default StaMPS processing, phase ramps are estimated for all slave images and subtracted from the deformation signal (see Fig. 5)

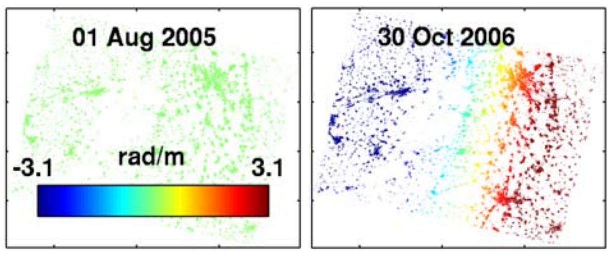

Figure 5. Phase ramp of interferogram using acquistions from 2005-08-01 (master) and 2006-10-30 (slave).

In Fig. 6 the result for LOS displacement rates from PS analysis are displayed before the slave contributions

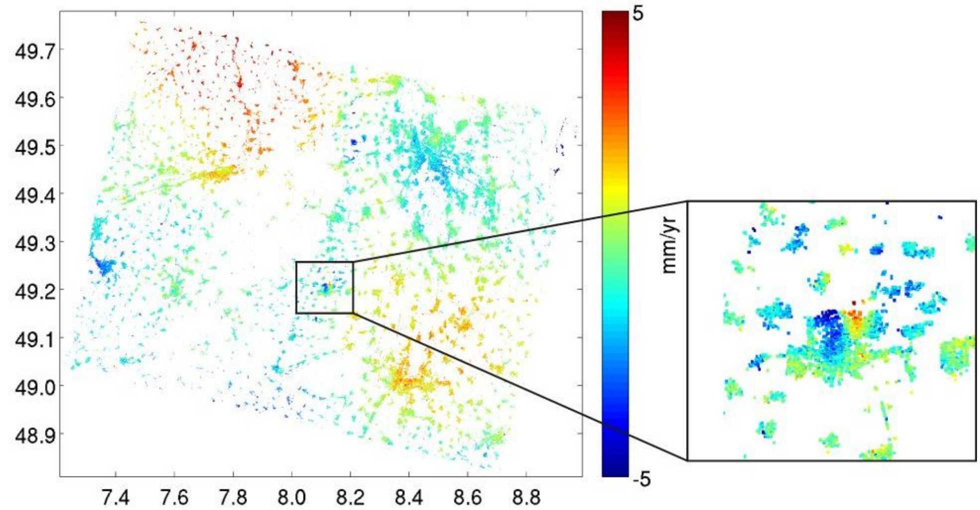

Figure 6. LOS displacement rates in the Northern URG without slave atmosphere estimation. The inset covers the city of Landau with the oil extraction field.

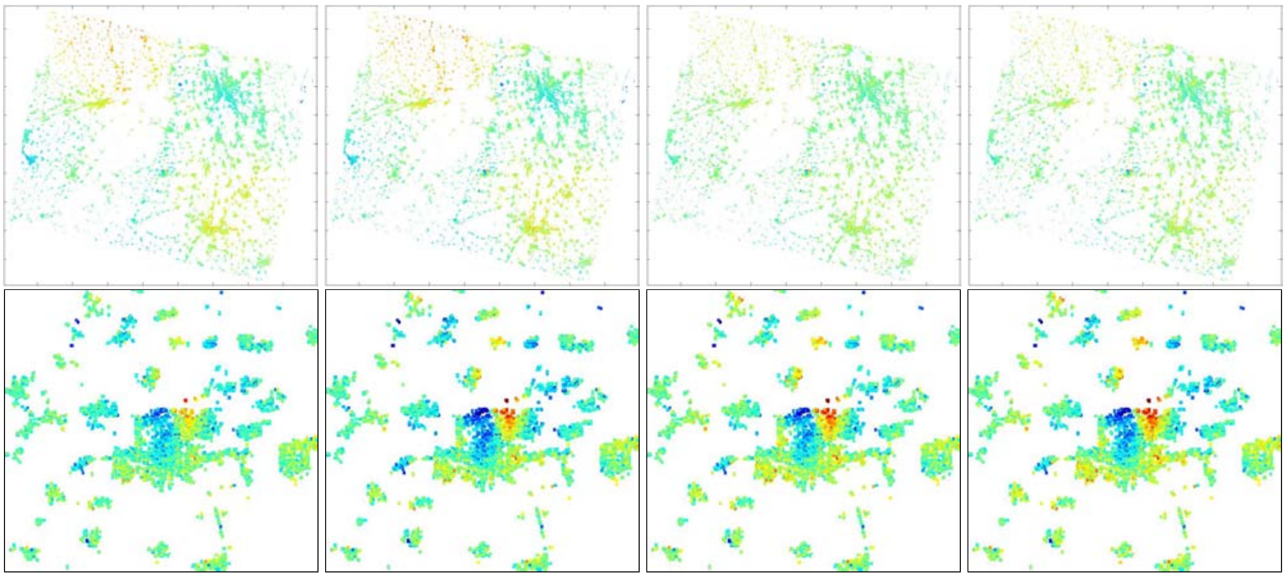

Figure 7. LOS displacement rates in the Northern URG (top) and zoomed into the Landau area (bottom) with slave atmosphere estimation using different parameter settings for spatially correlated filtering time window (tw) and minimum wavelength (mw), from left to right: tw = 365 d, mw = 100 m; tw = 365 d, mw = 1000 m; tw = 730 d, mw = 1000 m; tw = 730 d, mw = 2000 m. Same cut-out and colour scale as in Fig. 6.

to the spatially correlated phase are estimated and subtracted. Since the results from levelling indicate that the tectonic displacements are well below 1.0 mm/a, the large-scale displacements in Fig. 6 are supposed to be spatially correlated noise, e. g. due to atmospheric effects. Nevertheless the displacement caused by oil extraction close to Landau is clearly visible in the LOS displacement.

To reduce the spatial noise, the atmospheric signals are estimated by spatial filtering as described in [4]. As the default values for the spatial correlated filtering time window and minimum wavelength also subtract parts of the Landau deformation different settings for the two parameters are tested. Fig. 7 shows how the displacement estimates change for different parameter values in the whole scene (top) and the Landau deformation area (bottom). A larger minimum wavelength prevents the Landau deformation from being filtered out, whereas a larger time window reduces the spatially correlated noise. A time window of two years along with a minimum wavelength of 2 km turns out to provide a good solution for the filtering of spatially correlated nuisance terms without deteriorating the deformation signal.

In addition, ERS data were analysed in the same region using 56 scenes of ERS-1 and ERS-2 from 1992 to 2000. As the number of scenes is more than three times larger than for the Envisat case, the filtering of topographic, orbit and atmospheric phase terms gets more reliable in the ERS analysis. The separation of atmospheric nuisance terms by spatially correlated filtering was again performed using a time window of two years and a minimum wavelength of 2 km, whereas the magnitude of the filtered parts is much smaller for the ERS stack. The higher number of interferograms additionally results in a smaller mean standard deviation for LOS velocities from PS time series analysis in the ERS case (ERS: 0.3 mm/a; Envisat: 1.1 mm/a).

A comparison of both datasets shows a similar behavior of the resulting LOS velocities over large areas: Small uplift tendencies in the North Western part, subsidence in the area of Mannheim/Ludwigshafen. In contrast, the Landau deformation behaves significantly different for the ERS case, indicating that the deformation characteristics have changed over time. In Sect. 3.4 the ERS and Envisat LOS velocities are compared to the vertical components from levelling and GPS estimates. Especially from the levelling results the temporal change of the deformation characteristics is proved.

3.3. GNSS

The differential analysis of GNSS data delivers 3D displacement estimates, separated into Northing, Easting and Up components. Fig. 8 shows the coordinate time series for the GURN site located in the city of Landau. Jumps caused by a change of instrumentation at the sites are visible in the time series. The vertical displacement rate at site Landau is -2.6 mm/a for the period between 2004-01-01 and 2009-07-13 and +0.3 mm/a after an antenna change (2009-07-15). In our preliminary analysis only GPS observations are used. After a robust estimation of linear trends, horizontal and vertical displacement rates at GURN sites can be visualised as in [12].

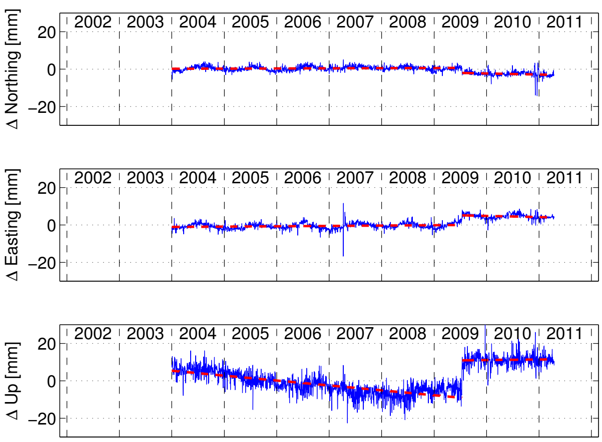

Figure 8. Time series of the local topocentric coordinate components (blue) for GURN site Landau. In addition, estimated regression lines (red) are shown.

3.4. Comparison

A comparison of results from different techniques is carried out for the time period from 2003 to 2009 in the area of the Landau deformation. Fig. 9 shows the results from InSAR (LOS), one GNSS site (Up component) and levelling (vertical velocities resulting from the analysis of the last three measurement epochs in Fig. 4).

The linear trend for the Up component of the GPS time series from 2004-01-01 to 2009-07-13 at site Landau is approx. -2.6 mm/a. The mean value of four adjacent levelling benchmarks with a spatial distance of 400 to 600 m to site Landau is -1.5 mm/a. The mean value of 35 adjacent PS points within a maximum distance of 250 m also yields -1.5 mm/a, revealing that the GPS estimate is slightly overrated. The InSAR LOS displacements match well with the displacement rates from levelling indicating that the major deformation is vertical. In the first period depicted in Fig. 9 (left) subsidences of -1 to -5 mm/a are visible within the oil fields. After 2000, the subsidence of the oil field north of Landau is shifted southwards showing magnitudes from -1 to -6 mm/a. In the area between the two oil fields an additional uplift signal is visible with magnitudes up to +7 mm/a.

The comparison obviously demonstrates the difference in the spatial resolution of the three techniques. The results from levelling alone cannot detect the uplift in the eastern part of the city of Landau, as no benchmarks are located there. On the other hand, the surface deformation in the fields north of Landau is not detected by InSAR as the PS points are restricted to urban areas. Therefore, a rigorous combination of the velocity estimates is desirable.

4. COMBINATION

Our research project aims for a combination of the three techniques in order to derive a 3D velocity field for the whole URG area. A joint interpretation however is challenging since each method relies on its own characteristics. Problems are inherent especially due to major differences in the temporal and spatial resolution and different time-dependent reference frames of the results. The advantages and disadvantages of the techniques are listed in the following:

InSAR:

+ Medium temporal resolution (months)
+ high spatial resolution (depending on coherence)
− LOS displacements (separation into horizontal and vertical components required)

GNSS:

+ high temporal resolution (permanent observations)
+ 3D analysis of displacements
− point-wise measurements with sparse spatial resolution (30-40 km distance between GNSS sites)

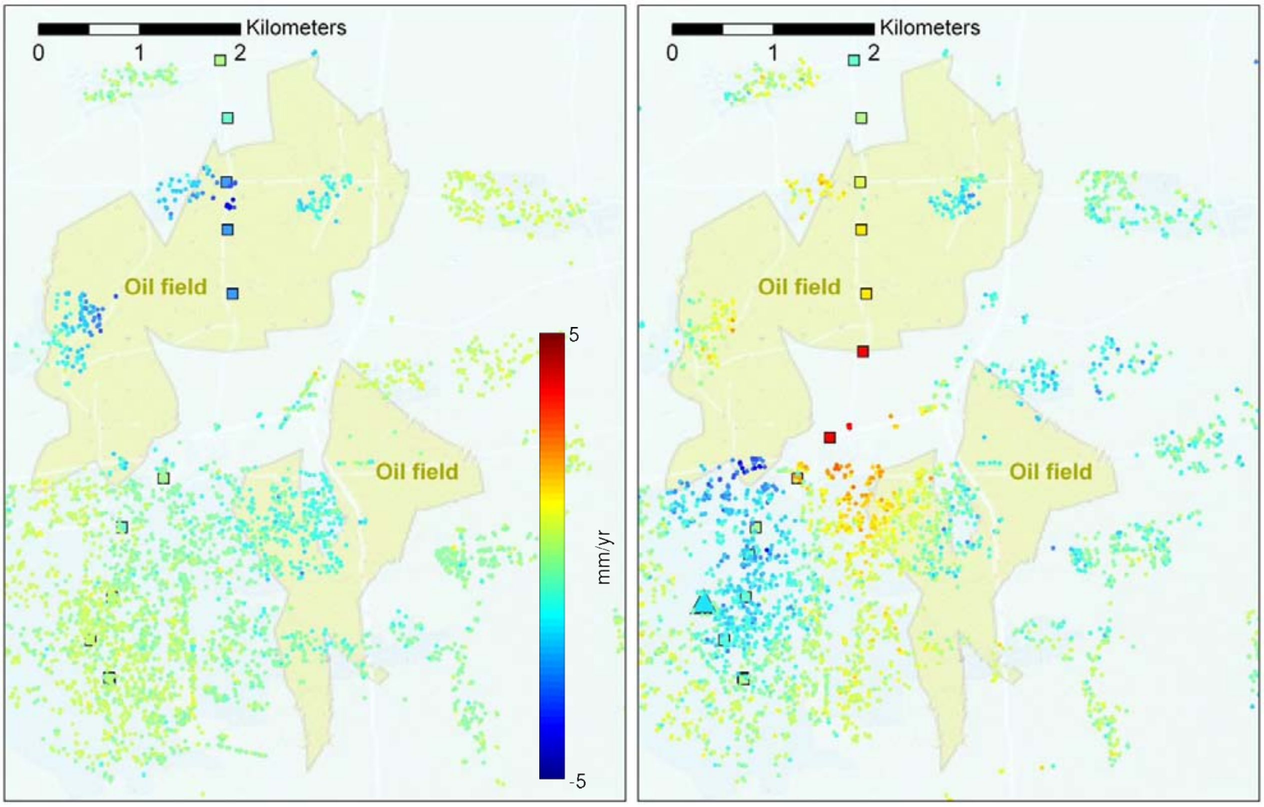

Figure 9. Oil fields close to Landau and deformations measured by InSAR, GPS and Levelling: LOS velocities at PS points (circles) with standard deviation < 0.5 mm/a estimated from ERS-1/2 data (1992-2000, left) and standard deviation < 1.5 mm/a estimated from Envisat data (2003-2008, right), vertical displacements at levelling benchmarks (squares) from two epochs (left: 1994 and 2003, right: 2003 and 2009) and linear trend of Up component for GNSS site Landau from 2004 to 2009 (triangle).

Levelling:

+ long timespan of available data (about 100 years)
+ most precise estimation of vertical displacements
− point-wise measurements along lines

For the fusion of the data we want to use the interpolation approach presented in [14] applying ordinary Kriging on the velocity estimates V_{LOS}, $V_{GNSS,x}$, $V_{GNSS,y}$, V_{Lev}. Second, the calculation of a 3D velocity field (v_x, v_y, v_z) is performed by analytical optimisation of Eq. 3 as described in [15] for InSAR and GPS measurements.

$$
\begin{aligned}
&U(v_x, v_y, v_z) = \\
&\sum_{i=1}^{N} \Bigg\{ \frac{1}{2\left(\sigma_{LOS}^i\right)^2}\left(V_{LOS}^i - S_x^i v_x - S_y^i v_y - S_z^i v_z\right)^2 \\
&+ \frac{1}{2\left(\sigma_{GNSS,x}^i\right)^2}\left(V_{GNSS,x}^i - v_x\right)^2 \\
&+ \frac{1}{2\left(\sigma_{GNSS,y}^i\right)^2}\left(V_{GNSS,y}^i - v_y\right)^2 \\
&+ \frac{1}{2\left(\sigma_{Lev}^i\right)^2}\left(V_{Lev}^i - v_z\right)^2 \Bigg\}
\end{aligned}
\tag{3}
$$

In addition, we integrate velocity estimates from the kinematic adjustment of levelling data and therefore neglect the Up component of GNSS sites. A comparison of vertical displacement rates between GNSS sites and adjacent levelling benchmarks in [12] has shown that the vertical rates from GPS data overrate the effective displacement since the temporal baseline is too short w.r.t. the magnitude of displacements. The LOS velocities from InSAR analysis have to be transformed to the local topocentric system using the corresponding unit vectors S_x^i, S_y^i, S_z^i pointing from the ground towards the SAR sensor.

5. CONCLUSIONS AND OUTLOOK

Within this paper, we presented our database, processing strategies and first results of a comprehensive analysis of crossborder geodetic data sets in the URG and surrounding regions. A kinematic adjustment of a transnational levelling network provides detailed insight into the vertical displacement field with accuracies better than 0.5 mm/a. In addition, local height comparisons along levelling lines resolve temporal features of a man-induced deformation. Continuous observations at permanent GNSS sites allow for an accurate estimation of the horizontal velocity field over large distances, albeit with a sparse spatial resolution. Finally, the analysis of InSAR acquisitions from ERS-1/2 and Envisat reveals LOS displacement rates at PS points at the mm-level.

Our research will be dedicated to further improvements in the velocity estimation from InSAR data. Therefore, investigations on orbit errors and atmospheric effects as well as on the combination of results from ERS and Envisat in the domain of PS time series will be carried out. For a rigorous combination of the three techniques a proper interpolation of the data on a common grid is indispensible along with weighting algorithms and outlier detection. The resulting 3D velocity field will contribute to an improved understanding of intraplate deformation processes and will deliver important boundary conditions for numerical geomechanical models. However, the geodetically observed surface displacements will always reflect a mixture of processes acting on different spatial and temporal scales (e. g., mining, groundwater withdrawal, natural hydrologic changes, glacial isostatic rebound, regional geochemical processes, tectonics) and have to be analysed appropriately.

ACKNOWLEDGMENTS

We thank our data providers for supplying GNSS and levelling data: RENAG (France), RGP (France), Teria (France), Orpheon (France), SAPOS® Baden-Württemberg (Germany), SAPOS® Rheinland-Pfalz (Germany), swisstopo (Switzerland), European Permanent Network, IGS, IGN (France), Landesamt für Geoinformation und Landmanagement (Baden-Württemberg, Germany), Landesamt für Vermessung und Geobasisinformation (Rheinland-Pfalz, Germany) and Landesamt für Kataster-, Vermessungs- und Kartenwesen (Saarland, Germany). We thank ESA for providing SAR data under the project ID 14193 and TU Delft for providing orbit files and the StaMPS software package. The project is funded through the German Science Foundation (DFG) under the grant HE 1433/17-2.

REFERENCES

1. F. Lemeille, M.E. Cushing, F. Cotton, B. Grellet, F. Menilletand J.-C. Audru, and F. Renardyand C. Flehoc. Evidence for Middle to Late Pleistocene faulting within the northern Upper Rhine Graben (Alsace Plain, France). *Comptes Rendus de l'Academie des Sciences Series IIA Earth and Planetary Science*, 328(12):839–846, 1999.
2. P. A. Ziegler. European Cenozoic rift system. *Tectonophysics*, 208:91 – 111, 1992.
3. M. Meghraoui, B. Delouis, M. Ferry, D. Giardini, P. Huggenberger, I. Spottke, and M. Granet. Active Normal Faulting in the Upper Rhine Graben and Paleoseismic Identification of the 1356 Basel Earthquake. *Science*, 293(5537):2070–2073, 2001.
4. A. Hooper, P. Segall, and H. Zebker. Persistent scatterer interferometric synthetic aperture radar for crustal deformation analysis, with application to Volcán Alcedo, Galápagos. *Journal of Geophysical Research: Solid Earth*, 112(B7), 2007.
5. Paul A. Rosen, Scott Hensley, Gilles Peltzer, and Mark Simons. Updated repeat orbit interferometry package released. *Eos, Transactions American Geophysical Union*, 85(5):47–47, 2004.
6. B. M. Kampes, R. F. Hanssen, and Z. Perski. Radar interferometry with public domain tools. In *Third International Workshop on ERS SAR Interferometry, FRINGE03, Frascati, Italy*, page 6 pp., 2003.
7. S. A. P. L. Cloetingh, et al. TOPO-EUROPE: the geoscience of coupled deep earth-surface processes. *Global and Planetary Change*, 58(1-4):1–118, 2007.
8. A. Knöpfler, F. Masson, M. Mayer, P. Ulrich, and B. Heck. GURN (GNSS Upper Rhine Graben Network) Status and First Results. 95th Journées Luxembourgeoises de Geodynamique, Echternach, Luxemburg, extended abstracts, 2009.
9. R. Dach, U. Hugentobler, P. Fridez, and M. Meindl. *User manual of the Bernese GPS Software Version 5.0*. Astronomical Institute, University of Bern, 2007.
10. J.-M. Nocquet and E. Calais. Crustal velocity field of western Europe from permanent GPS array solutions, 1996-2001. *Geophysical Journal International*, 154(1):72–88, 2003.
11. W. Dumouchel and F. O'Brien. Integrating a robust option into a multiple regression computing environment. In *Computer Science and Statistics: Proceedings of the 21st Symposium on the Interface*, pages 297–301. American Statistical Association, Alexandria, VA, 1989.
12. T. Fuhrmann, B. Heck, A. Knöpfler, F. Masson, M. Mayer, P. Ulrich, M. Westerhaus, and K. Zippelt. Recent surface displacements in the Upper Rhine Graben - Preliminary results from geodetic networks. *Tectonophysics*, 602(0):300 – 315, 2013.
13. K. Zippelt. *Modellbildung, Berechnungsstrategie und Beurteilung von Vertikalbewegungen unter Verwendung von Präzisionsnivellements*. Deutsche Geodätische Kommission, Reihe C, München, 1988.
14. M. C. Cuenca, R. Hanssen, A. Hooper, and M. Arikan. Surface Deformation of the Whole Netherlands After PSI Analysis. In *Proceedings Fringe 2011 Workshop, Frascati, Italy, 19-23 September 2011*, 2012.
15. J. Hu, J.J. Zhu, Z.W. Li, X.L. Ding, C.C. Wang, and Q. Sun. Robust Estimating Three-Dimensional Ground Motions from Fusion of InSAR and GPS Measurements. In *International Symposium on Image and Data Fusion (ISIDF), 2011*, pages 1–4, 2011.